Inorganic Chemistry, Vol. 14, No. 7, 1975 **1573**

Contribution from the Department of Chemistry,
University of British Columbia, Vancouver, Canada V6T 1W5

Orbital Ground States and Crystal Field Splittings in Some Octahedrally Coordinated High-Spin Ferrous Complexes

JOHN R. SAMS* and TSANG BIK TSIN

Received December 26, 1974 AIC408502

^{57}Fe Mössbauer spectra between 4 and 340°K and magnetic susceptibilities between 80 and 310°K have been recorded for three high-spin ferrous complexes of the type $FeL_6(ClO_4)_2$ [L = $(CH_3)_2SO$, $(C_6H_5)_2SO$, C_5H_5NO]. Signs of the quadrupole coupling constants e^2qQ and values of the asymmetry parameters η were obtained from magnetic perturbation Mössbauer measurements. Analyses of the temperature dependences of the quadrupole splittings in terms of a crystal field model yield values for the axial and rhombic field splitting terms and spin–orbit and spin–spin coupling constants. The values so deduced are shown to be consistent with the susceptibility data. The $(CH_3)_2SO$ and $(C_6H_5)_2SO$ complexes are tetragonally distorted, with $|xy\rangle$ ground states, whereas the C_5H_5NO derivative is trigonally distorted, with a ground state which is approximately the $[((2/3)^{1/2}|x^2-y^2\rangle - (1/3)^{1/2}|xz\rangle), ((2/3)^{1/2}|xy\rangle + (1/3)^{1/2}|yz\rangle)]$ orbital doublet. In no case is there a measurably large rhombic field, although the Jahn–Teller principle requires a nonaxial distortion in the C_5H_5NO complex. The C_5H_5NO derivative is found to show slow spin–lattice relaxation below ~30°K, and constitutes the first reported example of slow-relaxing Fe^{2+} ion in an approximately octahedral environment.

Introduction

In general, Mössbauer quadrupole splittings $|\Delta E_Q|$ in octahedral high-spin ferrous complexes show a continuous variation with temperature.[1,2] However, $Fe(H_2O)_6(ClO_4)_2$ was reported[3a] to show anomalous behavior in its Mössbauer spectrum. At 110°K $|\Delta E_Q|$ = 3.4 mm sec^{-1}, at 295°K the splitting was only 1.4 mm sec^{-1}, and between 220 and 250°K four lines were visible in the spectrum. These results were interpreted[3a] in terms of a tetragonal distortion with axial compression and an $|xy\rangle$ orbital ground state at low temperature, with a phase transition leading to axial elongation and a degenerate $(|xz\rangle + |yz\rangle)$ ground state at high temperature. A subsequent study of this compound using magnetic perturbation techniques[3b] indicated that the quadrupole coupling constant e^2qQ was negative at 5°K, so that the low-temperature ground state is $|z^2\rangle$ rather than $|xy\rangle$, and the distortion is trigonal rather than tetragonal. The predicted[3a] sign reversal was also confirmed,[3b] e^2qQ being positive at 296°K.

Reedijk and van der Kraan[4] have published Mössbauer data (at room temperature only) for five solvates of ferrous perchlorate of the type $FeL_6(ClO_4)_2$, where L was either a sulfoxide ligand or pyridine *N*-oxide. These data were interesting in that for four of the five complexes $|\Delta E_Q|$[5] was ca. 1.5 mm sec^{-1}, similar to the value found for the hexahydrate at the same temperature. On the other hand, for the dimethyl sulfoxide derivative $|\Delta E_Q|$ was reported to be 2.56 mm sec^{-1}. Reedijk and van der Kraan[4] suggested that the small splittings of ca. 1.5 mm sec^{-1} indicated "hardly distorted" octahedral cations, while the larger value for the $(CH_3)_2SO$ complex showed a greater distortion in this case. However, since distortions of comparable magnitude will produce a quadrupole splitting for an orbital singlet ground state which is roughly twice that for a doublet state, the alternative explanation of a different orbital ground state in the $(CH_3)_2SO$ derivative seemed to us equally plausible.

A more extensive investigation of such ferrous solvates was thus of interest for several reasons. First, there was the possibility that at low temperatures one might observe phase transitions of the type reported[3] for $Fe(H_2O)_6(ClO_4)_2$. Second, a detailed study of the temperature dependence of $|\Delta E_Q|$ in these derivatives, together with determinations of the signs of the electric field gradients (EFG's) at iron, would enable one to deduce the orbital ground states and to estimate the crystal field splitting parameters. Third, since crystal field parameters can also be estimated from the temperature dependence of the magnetic susceptibility, it was of interest to compare the results of two independent evaluations of these parameters.

This paper reports detailed magnetic susceptibility and ^{57}Fe Mössbauer measurements (the former between 80 and 310°K; the latter between 4.2 and 340°K) on three octahedral complexes of the type $FeL_6(ClO_4)_2$, where L = $(CH_3)_2SO$ (DMSO), $(C_6H_5)_2SO$ (DPSO), and C_5H_5NO (*N*-pyO).

Experimental Section

All reagents were obtained from commercial sources and used without further purification. The complexes were prepared by the method of Reedijk and van der Kraan[4] and identified by microanalyses and infrared spectra. Analyses were performed by Mr. P. Borda of this department. Ir spectra were recorded on a Perkin-Elmer 457 grating spectrophotometer, the Nujol mulls being held between CsI plates.

Magnetic susceptibilities were measured over the temperature range 80–310°K using a variable-temperature Gouy balance. All measurements were made at two field strengths and no field dependence was observed. The magnetic balance was calibrated with $Hg[Co(NCS)_4]$, and Pascal's constants were used to correct for diamagnetism.

The Mössbauer spectrometer consisted of an Austin Science Associates S-3 drive and linear motor, a Xe–CO_2 proportional counter, and a Nuclear-Chicago Model 24-2 analyzer operating in multiscalar mode. The ^{57}Co(Cu) source was maintained at ambient temperature, and the carefully powdered samples, contained in a copper cell with Mylar windows, were mounted in a Janis Model DT-6 variable-temperature cryostat. The cryostat was fitted with a Cryogenic Research Model TC-101 temperature controller, by means of which the temperature could be set and maintained constant to within less than ±0.02° throughout the data acquisition time. Temperatures were measured with calibrated Ge and Pt resistance thermometers.

For spectra recorded above room temperature the samples were mounted at the top of a solid copper rod which was wrapped with heating tape powered through a variable transformer. Temperatures were monitored with a copper–constantan thermocouple and were found to vary by less than ±0.5° during a run.

Mössbauer measurements in applied longitudinal magnetic fields of up to 50 kG were carried out in a Janis Model 11MDT helium cryostat fitted with a Westinghouse superconducting solenoid.[6] Owing to magnetic anisotropy effects discussed below, in order to determine the EFG signs unambiguously it was found necessary to heat the samples (which were located at the center of the applied field) to ca. 210–240°K while maintaining the solenoid at 4.2°K. The sample cell was fitted into a copper ring equipped with heater and thermocouple, and the entire sample chamber was evacuated to a pressure of less than 10^{-5} Torr. After transfer of liquid helium to the system, cryopumping was sufficient to prevent appreciable heat transfer from the sample to the solenoid helium bath.

Calibration of the velocity scale was effected with a metallic iron foil absorber. For spectra obtained in the absence of an applied field, the data points were least-squares fitted to lorentzian components,

Table I. Analytical Data and Important Ir Bands for $FeL_6(ClO_4)_2$ Complexes

L	% calcd C	H	N	Cl	% found C	H	N	Cl	ν(E–O),[a,b] cm^{-1}	ν(Fe–O),[b] cm^{-1}	ClO_4^- bands,[b] cm^{-1}
$(CH_3)_2SO$	19.90	4.98	0	9.83	19.79	4.94	0	9.76	990 vs, br	431 s 410 s	1085 vs, br 616 vs
$(C_6H_5)_2SO$	58.85	4.09	0	4.84	58.68	3.88	0		981 vs, br	419 w(?)	1082 vs, br 614 vs
C_5H_5NO	43.67	3.64	10.20	8.60	43.45	3.45	10.34	8.40	1217 s	307 s	1090 vs, br 617 vs

[a] E = S or N. [b] Key: s, strong; w, weak; v, very; br, broad.

Table II. Effective Magnetic Moments μ_{eff} of the $FeL_6(ClO_4)_2$ Complexes[a]

L = $(CH_3)_2SO$		L = $(C_6H_5)_2SO$		L = C_5H_5NO	
T, °K	μ_{eff}, BM	T, °K	μ_{eff}, BM	T, °K	μ_{eff}, BM
309.5	5.42	300.4	5.41	302.6	5.41
295.0	5.40	272.1	5.38	280.5	5.42
278.1	5.39	249.8	5.38	256.7	5.44
262.3	5.38	227.7	5.38	237.1	5.46
246.6	5.38	209.7	5.37	214.2	5.50
229.9	5.38	193.0	5.34	192.0	5.51
213.0	5.38	174.0	5.36	173.7	5.52
196.5	5.36	153.6	5.33	151.9	5.53
180.4	5.36	132.0	5.32	129.1	5.52
165.5	5.35	111.3	5.33	109.6	5.54
140.1	5.32	92.2	5.33	90.2	5.54
125.1	5.34	81.0	5.32	81.2	5.51
112.0	5.31				
97.0	5.33				
80.4	5.30				

[a] The μ_{eff} values are reproducible to within ±0.02 BM.

and no constraints were imposed on the fitting parameters. Isomer shifts are quoted relative to the centroid of the disodium pentacyanonitrosylferrate(II) spectrum.

Results and Discussion

General Comments. Analytical and ir data for the complexes are given in Table I. Only the structurally relevant ir bands have been listed, and agreement with previously published data[7-10] is generally good. In all three compounds only the ν_3 and ν_4 bands of the ClO_4^- ion are observed, showing that the anions retain tetrahedral symmetry and ruling out the possibility of iron–perchlorate coordination. The E–O stretching frequencies (E = S, N) are some 30–60 cm^{-1} lower in the complexes than in the free ligands, which indicates that the solvent molecules are coordinated to iron through the oxygen atoms. For the *N*-pyO complex ν(Fe–O) is seen at 307 cm^{-1}, and this band appears at ca. 400 cm^{-1} in the DMSO derivative. There is some uncertainty about the position of ν(Fe–O) in $Fe(DPSO)_6^{2+}$. Prabhakaran and Patel[10] have assigned this stretch to a weak band at 430 cm^{-1}, whereas for the other two complexes studied here ν(Fe–O) appears as a strong absorption. However, the only other band in the 600–250-cm^{-1} region in $Fe(DPSO)_6^{2+}$ not attributable to a ligand mode is a strong band at 260 cm^{-1}, which seems too low in comparison with ν(Fe–O) for the other sulfoxide complexes.[11]

Data for the effective magnetic moments μ_{eff} appear in Table II and clearly indicate that the three complexes are high spin (S = 2). All values fall in the rather narrow range 5.30–5.54 BM, and there is little variation among the three solvates. This suggests, contrary to the conclusions of Reedijk and van der Kraan,[4] that the magnitudes of the axial distortions in all the complexes are quite similar. Although the μ_{eff} values do not have a pronounced temperature dependence, it can be seen that for the DMSO and DPSO derivatives μ_{eff} decreases smoothly with decreasing temperature, while the values for the *N*-pyO complex increase initially before showing a slight decline at low temperature. As we shall see below, this difference in the behavior of μ_{eff} as a function of temperature presumably arises from the fact that the DMSO and DPSO complexes have different orbital ground states from that of the *N*-pyO derivative.

Table III. ^{57}Fe Mössbauer Parameters for the $FeL_6(ClO_4)_2$ Complexes[a]

L = $(CH_3)_2SO$			L = $(C_6H_5)_2SO$			L = C_5H_5NO		
T, °K	δ, mm sec^{-1}	ΔE_Q, mm sec^{-1}	T, °K	δ, mm sec^{-1}	ΔE_Q, mm sec^{-1}	T, °K	δ, mm sec^{-1}	ΔE_Q, mm sec^{-1}
316.0	1.51	2.52	331.0	1.49	2.50	333.6	1.41	1.62
295.5	1.52	2.71	315.5	1.50	2.58	318.5	1.43	1.63
295.2	1.52	2.72	294.8	1.51	2.68	294.9	1.44	1.64
273.0	1.54	2.86	265.0	1.55	2.87	273.1	1.46	1.66
250.0	1.55	2.92	235.0	1.56	2.99	250.0	1.47	1.67
220.0	1.57_5	3.02	205.0	1.58	3.10	190.0	1.50	1.71
190.1	1.58_5	3.08	175.0	1.59	3.19	159.9	1.52	1.74
160.0	1.60	3.12	145.0	1.60	3.28	130.2	1.53	1.76
131.0	1.61_5	3.15	114.7	1.61	3.34	100.0	1.54	1.79
115.1	1.63	3.17	95.1	1.62	3.37	83.7	1.55	1.81
100.0	1.63	3.17	85.0	1.63	3.37	82.1	1.54	1.81
82.5	1.63	3.18	82.7	1.62_5	3.22	81.0	1.55	1.82
81.8	1.63	3.19	60.0	1.63	3.36	65.0	1.55_5	1.85
60.0	1.63	3.19	30.0	1.63_5	3.36	40.0	1.55	1.87
40.0	1.63_5	3.20	8.8	1.63	3.37	30.1	1.56	1.89
15.0	1.64	3.19				25.0	1.56	1.90
7.9	1.64_5	3.22				20.0	1.56_5	1.90
						15.0	1.57	1.91
						11.0	1.57	1.93
						9.0	1.56	1.91
						8.2	1.56	1.92

[a] Isomer shifts are quoted relative to sodium nitroprusside. Error limits for both δ and ΔE_Q are estimated to be +0.01 mm sec^{-1}.

Mössbauer isomer shifts, δ, and quadrupole splittings, $|\Delta E_Q|$, are listed in Table III. Our results for the DMSO and *N*-pyO complexes are in only moderately good agreement with those of Reedijk and van der Kraan.[4] (The DPSO derivative was not reported in ref 4.) In particular, the "room-temperature" $|\Delta E_Q|$ values reported by these authors[4] are between 0.08 and 0.16 mm sec^{-1} smaller than our values at 295°K. We have repeated our measurements on several different samples of each compound, and they are certainly accurate.

The δ values in Table III lie within the range normally observed for octahedral S = 2 ferrous complexes and show little variation from one solvate to another. This implies that the extent of covalency of the Fe–O bonds is probably very similar in all these derivatives. The temperature dependence of the δ values can be attributed to a second-order Doppler shift and will not be considered further.

The quadrupole splitting data show marked differences, both in temperature dependence and in the magnitude at a given temperature. At 295°K the *N*-pyO complex has a splitting of 1.64 mm sec^{-1}, whereas for the other two derivatives the splittings are ca. 2.7 mm sec^{-1}. The latter complexes also show a more pronounced temperature dependence of $|\Delta E_Q|$, and it is clear that on the basis of Mössbauer data the compounds divide into the same groups as noted above in connection with the magnetic moments.

In no case was a four-line spectrum observed, and we could find no indication in any of these complexes of the type of phase transition reported[3] for $Fe(H_2O)_6(ClO_4)_2$.

Orbital Ground States of the Complexes. An octahedral crystal field splits the ferrous 3d orbitals into triply degenerate t_{2g} and doubly degenerate e_g subsets, with the triplet lying lower by an energy $10Dq$. If the fourfold axis C_4 is taken as the quantization axis, the d orbitals transform as

$$e_g = |x^2 - y^2\rangle, |z^2\rangle$$

$$t_{2g} = |xy\rangle, |xz\rangle, |yz\rangle$$

On the other hand, if C_3 (lying along the [111] direction of the octahedron) is assumed to be the axis of quantization, then in terms of the conventional real d orbitals one has instead[13]

$$e_g = \begin{cases} (1/3)^{1/2}|x^2 - y^2\rangle + (2/3)^{1/2}|xz\rangle \\ (1/3)^{1/2}|xy\rangle - (2/3)^{1/2}|yz\rangle \end{cases}$$

$$t_{2g} = \begin{cases} |z^2\rangle \\ (2/3)^{1/2}|x^2 - y^2\rangle - (1/3)^{1/2}|xz\rangle \\ (2/3)^{1/2}|xy\rangle + (1/3)^{1/2}|yz\rangle \end{cases}$$

An axial field partially lifts the degeneracy of the t_{2g} orbitals,[14] splitting them into a doublet and a singlet separated by $3Ds$. In the tetragonal (C_4) case the singlet is $|xy\rangle$ and in the trigonal (C_3) case it is $|z^2\rangle$. If there is also a rhombic field, the remaining spatial degeneracy of the t_{2g} orbitals is removed, the doublet being split by $12Dr$. However, since both the sign of ΔE_Q and magnitude of the asymmetry parameter η are independent of the sign of Dr we cannot tell, in the tetragonal plus rhombic case, for example, whether $|xz\rangle$ or $|yz\rangle$ lies lower. Each of the 3d wave functions also has a fivefold spin degeneracy which will be split by the spin–orbit coupling, but for the moment we ignore this feature since we are interested here only in the orbital ground state.

The contribution to the EFG from a single electron in each of the d orbitals is[15] $+4/7e\langle r^{-3}\rangle$ for $|xy\rangle$ and $|x^2 - y^2\rangle$, $-4/7e\langle r^{-3}\rangle$ for $|z^2\rangle$, and $-2/7e\langle r^{-3}\rangle$ for $|xz\rangle$ and $|yz\rangle$, where $\langle r^{-3}\rangle$ is the expectation value of $1/r^3$ for the 3d radial function. It therefore follows that for similar values of Ds an orbitally nondegenerate ground state should produce an appreciably larger quadrupole splitting than that for a doublet state. It is possible, of course, for an orbital singlet ground term to produce only a small $|\Delta E_Q|$ at room temperature if $|3Ds|/k$ is not much larger than 300°K, since this would provide significant thermal population of the doublet. However, $|\Delta E_Q|$ would then be expected to show a very pronounced increase on lowering the temperature, as the electron is progressively localized in the singlet. Finally, since an EFG of $^4/_7e\langle r^{-3}\rangle$ is expected to yield a quadrupole splitting of about 4 mm sec^{-1}, experimental $|\Delta E_Q|$ values substantially greater than 2 mm sec^{-1} are only consistent with a singlet ground state.

From this discussion and the data in Table III it is clear that for both the $Fe(DMSO)_6^{2+}$ and $Fe(DPSO)_6^{2+}$ complexes the ground state must be an orbital singlet, whereas $Fe(N\text{-}pyO)_6^{2+}$ has a doublet ground state. To identify these states more precisely we must know the sign of V_{zz}, the principal component of the EFG tensor. For a paramagnetic complex, however, there are certain difficulties associated with the usual magnetic perturbation method[6,16] for determining the sign of V_{zz}. In the presence of an external magnetic field H_{ext}, the effective field at the nucleus can be written as[17]

$$H_{eff} = H_{ext} + (\langle S\rangle/S)H_n^{(0)} \quad (1)$$

where H_n^0 is the saturation value of the internal magnetic field at the nucleus and $\langle S\rangle$ is the thermal average of the total electronic spin. At low temperatures where the susceptibility is large, H_{eff} can be very different from H_{ext}. The situation is further complicated by the facts that (a) both the magnetization and hyperfine field tensors are anisotropic for high-spin Fe^{2+} and (b) for a polycrystalline sample the magnitude of the splittings is an average over all possible orientations of H_{ext} relative to the z axis of the EFG.

These difficulties can be overcome by maintaining the specimen at high temperature so that the magnetization $\langle S\rangle$ produced by the applied field is negligible and $H_{eff} \simeq H_{ext}$. The situation is then similar to that for a diamagnetic complex,[6] where the line of the quadrupole doublet which arises from the $|\pm^1/_2\rangle \rightarrow |\pm^1/_2\rangle$ nuclear spin transitions splits into an apparent triplet, and that from the $|\pm^1/_2\rangle \rightarrow |\pm^3/_2\rangle$ transitions splits into a doublet. To ensure that our results would be unambiguous, determinations of the sign of V_{zz} in the three complexes were made with the samples at 210°K or higher in applied fields of 35–50 kG.

In each case we find $V_{zz} > 0$. This is an important and surprising result because it shows there are two fundamentally different types of distortions from octahedral symmetry in these solvates. For the DMSO and DPSO complexes the ground state is $|xy\rangle$ and the distortion is a compression along the tetragonal C_4 axis. For the N-pyO derivative the ground state is essentially the doublet $[((2/3)^{1/2}|x^2 - y^2\rangle - (1/3)^{1/2}|xz\rangle), ((2/3)^{1/2}|xy\rangle + (1/3)^{1/2}|yz\rangle)]$, and the distortion corresponds to an elongation along the trigonal C_3 axis.

The reasons for the occurrence of two distinct types of distortions in these complexes are not completely clear but may well arise from different steric requirements of the ligands. The most obvious difference is that N-pyO contains a heterocyclic ring which is only two bonds removed from the Fe^{2+} ion in the complex, whereas DMSO and DPSO do not. Since the Fe–O–N bond angles are expected to be roughly 120°,[18-20] the presence of six rings of substantial size in close proximity to the central ion should produce considerable steric crowding. Molecular models suggest that this is indeed so. DMSO is of course the least bulky of the ligands, but even for the DPSO complex, since the phenyl rings are one bond (about 1.8 Å) farther away from the ferrous ion than are the heterocycles in the N-pyO derivative, the structure appears to be less crowded. It is worth noting here that the X-ray crystal structure of $(CH_3)_2SnCl_2 \cdot 2N\text{-}pyO$[18] shows the N-pyO groups to be trans, whereas the DMSO ligands are cis in $(CH_3)_2SnCl_2 \cdot 2DMSO$.[19]

Crystal Field, Spin–Orbit, and Spin–Spin Splitting Parameters. Both Ingalls[2] and Gibb[21] have treated the effects of crystalline fields and spin–orbit coupling on the quadrupole splitting in octahedral Fe^{2+} systems, and we have followed these treatments in general outline. The effect of the noncubic part of the crystal field is treated in terms of the perturbation Hamiltonian

$$\mathcal{H} = V_T + V_R + V_{SO} + V_{SS} \quad (2)$$

where V_T is the axial (tetragonal or trigonal) field term, V_R the rhombic term, V_{SO} the spin–orbit coupling, and V_{SS} the intraionic spin–spin coupling. The last term was omitted by both Ingalls[2] and Gibb[21] and has little effect when fitting ΔE_Q vs. T data recorded at 80°K and above. However, its inclusion significantly improves agreement between calculated ΔE_Q values and our low-temperature data in the 8–40°K region. In fact, for the range of axial distortions encountered here, omission of V_{SS} from the Hamiltonian causes $|\Delta E_Q|$ to decrease rather than increase as the temperature is lowered below ~80°K, contrary to what is observed.

In operator notation eq 2 can be written as[13,22]

$$\mathcal{H} = Ds(\hat{L}_z^2 - 2) + Dr(\hat{L}_+^2 + \hat{L}_-^2) - \lambda[\hat{L}_z\hat{S}_z + {}^1/_2(\hat{L}_+\hat{S}_- + \hat{L}_-\hat{S}_+)] - D\sigma(S_z^2 - 2) \quad (3)$$

where the $\hat{L}_i$ and $\hat{S}_i$ are respectively orbital and spin angular momentum shift operators, Ds and Dr the axial and rhombic

field parameters, and λ and $D\sigma$ the spin–orbit and spin–spin coupling constants. The Hamiltonian of eq 3 operates on an appropriate set of n 3d wave functions. Optical spectra of the present compounds[4] show that the cubic field splittings $10Dq$ are in the range 9300–10,000 cm^{-1}. Thus there will be no appreciable admixture of t_{2g} and e_g orbitals under our experimental conditions. In order to lessen the computation times required we have therefore omitted the e_g orbitals in our calculations (hence the absence of the cubic field term V_0 in $\mathcal{H}$). This allows us to truncate the 25 × 25 matrices to 15 × 15 matrices which contain only the t_{2g} set of orbitals. Some preliminary calculations were performed using a full orbital set to test the validity of this truncation, and we found no significant difference between the results of the 15 × 15 and 25 × 25 matrix diagonalizations.

For the trigonally distorted complex the basis set of 15 t_{2g} wave functions used was

$$|2,0\rangle|M_S\rangle$$

$$(2/3)^{1/2}|2,\pm2\rangle \mp (1/3)^{1/2}|2,\mp1\rangle)|M_S\rangle$$

where in the $|L, M_L\rangle|M_S\rangle$ notation, M_L is the z component of the total orbital angular momentum L, and $M_S = 0, \pm1, \pm2$ is the z component of spin angular momentum. For tetragonal distortions the corresponding basis set was

$$1/2^{1/2}(|2,2\rangle - |2,-2\rangle)|M_S\rangle$$

$$1/2^{1/2}(|2,1\rangle \pm |2,-1\rangle)|M_S\rangle$$

The quantities Ds/λ, Dr/λ, and $D\sigma/\lambda$ were treated as independent parameters which were read into the computer. The matrix was then diagonalized to obtain the eigenvalues ϵ_i/λ and corresponding eigenvectors $|i\rangle$, which were subsequently used to calculate the quadrupole splittings and magnetic moments.

The contributions to the nine components V_{kl} ($k, l = x, y, z$) of the EFG tensor were calculated for each eigenvector $|i\rangle$, and the ensemble averages

$$Z^{-1}\sum_{i=1}^{15}\langle i|V_{kl}/e|i\rangle \exp(-\epsilon_i/kT)$$

were formed. $Z = \sum\exp(-\epsilon_i/kT)$ is the partition function. The EFG matrix was diagonalized to obtain the tensor elements in the principal axis system. The quadrupole splitting can be written as

$$\Delta E_Q = {}^1/_2e^2Q(1-R)[q^2 + {}^1/_3(\eta q)^2]^{1/2} \quad (4)$$

$$= {}^1/_2e^2Q(1-R)({}^4/_7\langle r^{-3}\rangle)(F_q{}^2 + {}^1/_3F_{\eta q}{}^2)^{1/2} \quad (5)$$

where eQ is the nuclear quadrupole moment, $(1 - R)$ is the Sternheimer correction for core polarization, and F_q and $F_{\eta q}$ are given in terms of the principal components of the EFG by[2]

$$F_q = ({}^4/_7\langle r^{-3}\rangle Z)^{-1}\sum_i\langle i|V_{zz}/e|i\rangle \exp(-\epsilon_i/kT) \quad (6)$$

$$F_{\eta q} = ({}^4/_7\langle r^{-3}\rangle Z)^{-1}\sum_i\langle i|(V_{xx} - V_{yy})/e|i\rangle \exp(-\epsilon_i/kT) \quad (7)$$

The quantity ${}^2/_7e^2Q(1 - R)\langle r^{-3}\rangle$ has been estimated[2,23] to have a numerical value of ca. 4.1 mm sec^{-1}, whence

$$\Delta E_Q = 4.1(F_q{}^2 + {}^1/_3F_{\eta q}{}^2)^{1/2} \text{ mm sec}^{-1} \quad (8)$$

For various choices of the splitting parameters Ds, Dr, $D\sigma$, and λ, eq 8 was used to generate curves of ΔE_Q as a function of T which were then compared with the experimental curves.

The effective magnetic moment μ_{eff} can be calculated from the eigenvectors and eigenvalues obtained above, using second-order perturbation theory.[13,24] The susceptibility χ_k in a particular direction ($k = x, y, z$) is given by

$$\chi_k = N_0Z^{-1}\Sigma\{[W_{i,k}^{(1)}]^2/kT - 2W_{i,k}^{(2)}\} \exp(-\epsilon_i/kT) \quad (9)$$

Table IV. Crystal Field Parameters Derived from Quadrupole Splitting Data[a]

Compd	$3Ds$, cm^{-1}	λ, cm^{-1}	$D\sigma$, cm^{-1}	κ[b]
$Fe(DMSO)_6(ClO_4)_2$	500	103	28	0.89
$Fe(DPSO)_6(ClO_4)_2$	475	90	23	0.90
$Fe(N\text{-}pyO)_6(ClO_4)_2$	455	80	24	0.94

[a] In every case we have assumed the rhombic field term $Dr = 0$. [b] Orbital reduction factor derived by fitting magnetic moment data, using Ds, λ, and $D\sigma$ values obtained from Mössbauer data.

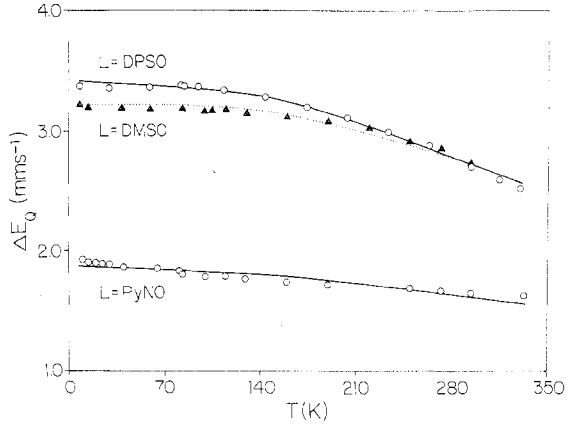

Figure 1. Comparison of observed and calculated quadrupole splittings as a function of temperature for the three $FeL_6(ClO_4)_2$ complexes. The parameter values employed to generate the theoretical curves are listed in Table IV.

where

$$W_{i,k}^{(1)} = \langle i|\hat{\mu}_k|i\rangle \quad (10)$$

$$W_{i,k}^{(2)} = \sum_{j\neq1}|\langle i|\hat{\mu}_k|j\rangle|^2/(\epsilon_i - \epsilon_j) \quad (11)$$

$$\hat{\mu}_k = -\beta(\kappa\hat{L}_k + 2\hat{S}_k) \quad (12)$$

N_0 is Avogadro's number, β the Bohr magneton, and κ the orbital reduction factor. The corresponding magnetic moment in the k direction is

$$\mu_k = (3kT\chi_k/N_0)^{1/2} \quad (13)$$

and the effective moment is then obtained as

$$\mu_{eff} = {}^1/_3(\mu_x{}^2 + \mu_y{}^2 + \mu_z{}^2)^{1/2} \quad (14)$$

In order to deduce crystal field parameters from the Mössbauer data via eq 8, we proceeded as follows. For all the compounds the spectra obtained in applied magnetic fields indicated that $\eta \simeq 0$, so that the EFG's have effectively axial symmetry, and we accordingly set $Dr = 0$. We also imposed the restriction $70 < \lambda < 103$ cm^{-1}, and theoretical curves were plotted in the form ΔE_Q vs. kT/λ. Comparison of such curves, calculated for several different ranges of parameter values, with the experimental data then provided reasonable first estimates of Ds, $D\sigma$, and λ. Since changes in these three parameters affect the computed curves in rather different ways (vide infra and ref 21), it is relatively straightforward to decide the direction in which one's first estimates should be varied, and at this point we adopted least-squares techniques to refine the parameter values. λ was allowed to vary in steps of ±5 cm^{-1}, $3Ds$ in steps of ±10 cm^{-1}, and $D\sigma$ in steps of ±2 cm^{-1}. Within these step limitations "best fit" sets of Ds, $D\sigma$, and λ values (as judged by standard deviations) were obtained, and these appear in Table IV. Figure 1 compares the experimental quadrupole splitting data with theoretical curves computed from these parameter values.

Owing to the small temperature dependence of μ_{eff} for all three complexes and to the fact that our measurements do not

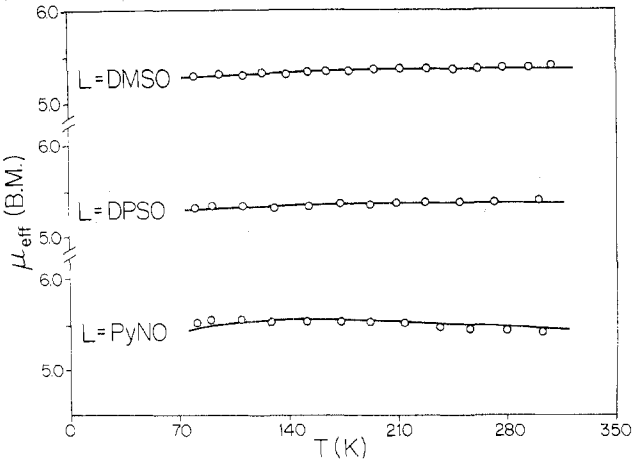

Figure 2. Comparison of observed and calculated effective magnetic moments as a function of temperature for the $FeL_6(ClO_4)_2$ complexes. The parameters used to compute the theoretical points appear in Table IV.

extend below 80°K, it was clearly impractical to try to estimate all the quantities Ds, $D\sigma$, λ, and κ from these data. We therefore employed the values of Ds, $D\sigma$, and λ obtained from fitting the Mössbauer results and fitted the μ_{eff} vs. T data merely by adjusting κ. In each case the value of κ so found is about 0.9, which seems very reasonable for complexes of this type. It can be seen from Figure 2 that the fit of the data is certainly adequate, so that the μ_{eff} values are fully consistent with the parameters listed in Table IV.

It will be appreciated that the crystal field treatment we have employed is only approximate, and the derived splitting parameters should be viewed accordingly. However, several comments on our results are appropriate here. First, one sees that the magnitudes of the axial fields are very similar for the three solvates despite the fact that the ΔE_Q values show marked differences. This is, of course, a consequence of the different orbital ground states, but clearly illustrates that it is quite inappropriate to argue about the magnitude of the crystal field splitting in a compound on the basis of a single measurement of ΔE_Q.

Second, with the exception of the DMSO complex the λ values are about 80–90% of the free-ion value ($\lambda_0 = 103$ cm^{-1}), suggesting a slight radial expansion of the ferrous 3d orbitals.[25] We were unable to obtain a satisfactory fit of the data for $Fe(DMSO)_6(ClO_4)_2$ using a λ value less than 100 cm^{-1}, which implies very little if any radial expansion in this case.

The spin–spin coupling term, $D\sigma(S_z^2 - 2)$, was introduced here to account for the low-temperature behavior of ΔE_Q. An examination of Gibb's results,[21] in which this term was omitted, shows that for the parameter ranges 100 cm^{-1} < Ds < 300 cm^{-1} and 60 cm^{-1} < λ < 100 cm^{-1} which are appropriate here, the ΔE_Q vs. T curves exhibit maxima, and a decline in ΔE_Q at low temperature is predicted. This behavior is not observed for any of our three complexes. Rather we find that below 80°K ΔE_Q is effectively constant for the DMSO and DPSO derivatives and continues to increase for the N-pyO complex. This temperature dependence cannot be duplicated in the theoretical curves unless the $D\sigma$ term is included. The values of about 20–30 cm^{-1} found here for $D\sigma$ are probably reasonable since for other transition metal ions ESR measurements yield values less than 100 cm^{-1} in most cases.

The fact that the magnetic perturbation spectrum of $Fe(N\text{-pyO})_6(ClO_4)_2$ gives no indication of a nonzero η (see Figure 3) raises an interesting question. Since Kramers' theorem does not apply to even-electron systems, a nondegenerate orbital ground state is demanded by the Jahn–Teller principle. Furthermore, neither spin–orbit nor spin–spin coupling lifts

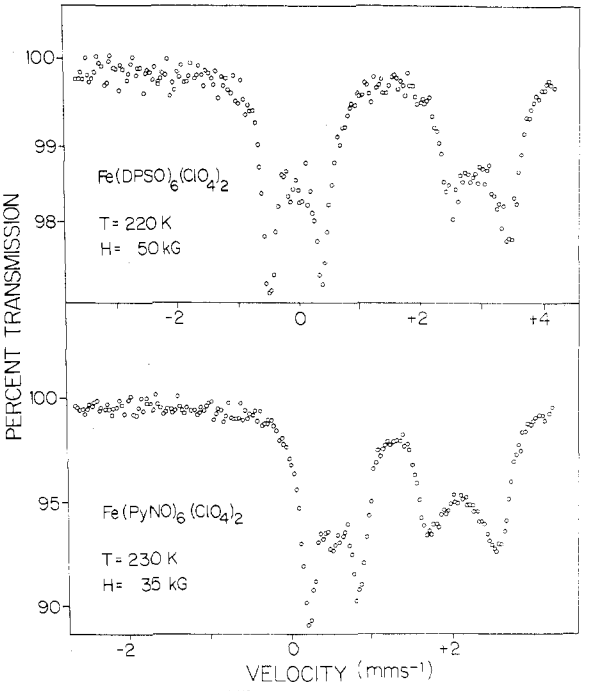

Figure 3. Mössbauer spectra in longitudinal applied magnetic fields: (top) $Fe(DPSO)_6(ClO_4)_2$ at 220°K and $H_{ext} = 50$ kG; (bottom) $Fe(N\text{-pyO})_6(ClO_4)_2$ at 230°K and $H_{ext} = 35$ kG. In both cases $e^2qQ > 0$ and $\eta \simeq 0$.

the orbital degeneracy, and we therefore see that unless the ground state is either $|xy\rangle$ or $|z^2\rangle$, there should be a Jahn–Teller-induced rhombic distortion to produce a singlet ground state. This would, of course, lead to a nonaxially symmetric EFG and a nonzero η. Measurements at 4.2°K in applied magnetic fields, which will be reported elsewhere, enable us to place an upper limit of about 15 cm^{-1} for any Jahn–Teller distortion in this complex. A splitting of this magnitude would give $\eta \simeq 0.1$, which is too small to have an observable effect on the spectrum of Figure 3b.

Slow Spin–Lattice Relaxation and Paramagnetic Hyperfine Splitting. In the absence of cooperative effects, spin–lattice relaxation of Fe^{2+} is usually rapid. Ingalls[2] has estimated the relaxation time for Fe^{2+} in an approximately octahedral environment as about 10^{-9}–10^{-11} sec, much shorter than the nuclear Larmor precession time. Thus, if a ferrous complex is still paramagnetic down to very low temperatures, its Mössbauer spectrum is expected to remain a sharp doublet, and in the absence of an applied field no magnetic hyperfine structure will be observed.

Typical of such fast-relaxing paramagnets are the $Fe(DMSO)_6(ClO_4)_2$ and $Fe(DPSO)_6(ClO_4)_2$ complexes. As shown in Figure 4 the spectra of both compounds are sharp quadrupole doublets down to ca. 8°K, and there is no evidence of paramagnetic hyperfine splitting. Similar results were reported[3b] for $Fe(H_2O)_6(ClO_4)_2$ at 5°K. However, very different behavior is observed for $Fe(N\text{-pyO})_6(ClO_4)_2$, where below 30°K the lines broaden asymmetrically (see Figure 5). Although there are several possible mechanisms for asymmetric line broadening in Mössbauer spectra of randomly oriented polycrystalline samples,[26–30] the only one consistent with the temperature dependence found here is an increase in the spin–lattice relaxation time at low temperature, leading to an onset of paramagnetic hyperfine splitting. At 4.2°K the asymmetry is slightly greater than in the 8.2°K spectrum shown in Figure 5, but the hyperfine splitting is still unresolved. This appears to be the first example of this effect in an approximately octahedral ferrous complex.[31] The only other cases of slow-relaxing Fe^{2+} reported thus far are in the mineral

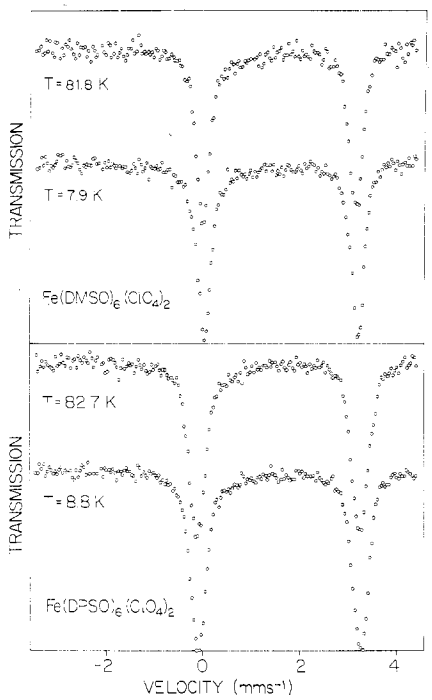

Figure 4. Zero-field Mössbauer spectra of (top) $Fe(DMSO)_6(ClO_4)_2$ at 81.8 and 7.9°K and (bottom) $Fe(DPSO)_6(ClO_4)_2$ at 82.7 and 8.8°K. Note the absence of line broadening at low temperatures.

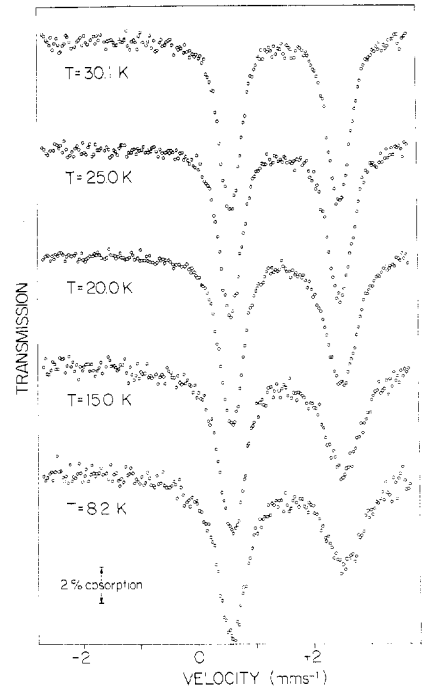

Figure 5. Mössbauer spectra of $Fe(N\text{-pyO})_6(ClO_4)_2$ between 30.1 and 8.2°K. Sample temperatures are indicated on the figure. At 30.1°K the line widths are equal within experimental error, whereas at 8.2°K, $\Gamma_2 = 1.44\Gamma_1$. The asymmetric line broadening results are from slow spin-lattice relaxation.

gillespite ($BaFeSi_4O_{10}$)[26,32] and the tetrakis(1,8-naphthyridine) complex $Fe(C_8H_6N_2)_4(ClO_4)_2$.[33] In the former the ferrous ions are in a square-planar environment of oxygens, while in the latter they are octacoordinate, both arrangements being quite unusual for Fe^{2+}.

From Griffith's[34,35] results for even-electron systems, one expects that the line of the quadrupole doublet arising from the $|\pm^1/_2\rangle \rightarrow |\pm^3/_2\rangle$ nuclear spin transitions will broaden before the $|\pm^1/_2\rangle \rightarrow |\pm^1/_2\rangle$ line as the relaxation rate decreases. This is because the lowest spin–orbit-split state is a doublet which has an effective hyperfine field parallel to the trigonal z axis.[35,36] If the fluctuations are sufficiently slow so that this effective field H_{eff} is not time averaged to zero, the $|\pm^3/_2\rangle$ excited state will be split by 3α whereas the $|\pm^1/_2\rangle$ state is split only by an amount α ($\alpha = g_1\beta_n H_{eff}$, where g_1 is the gyromagnetic ratio for the excited state and β_n the nuclear magneton).[37] The magnetic perturbation spectrum shown in Figure 3 confirms that the broad high-velocity line corresponds to the $|\pm^1/_2\rangle \rightarrow |\pm^3/_2\rangle$ transitions.

The factors responsible for the slow relaxation observed for the *N*-pyO complex are not clear at this time. We suspect the factor of primary importance is that the orbital ground state is nearly degenerate, which could have a significant effect on the orbit–lattice coupling coefficients. Detailed studies of the behavior of these complexes in applied magnetic fields at low temperatures are under way and will be reported in the near future.

Acknowledgment. We thank Dr. M. G. Clark for an interesting discussion of the slow relaxation. We are grateful to Mrs. A. Sallos and Mr. M. Vagg for technical assistance and to Beatrice Krizan for drawing the figures. This work was supported in part by the National Research Council of Canada, and T.B.T. thanks the NRC for the award of a postgraduate fellowship.

Registry No. $Fe(DMSO)_6(ClO_4)_2$, 16742-95-3; $Fe(DPSO)_6(ClO_4)_2$, 13963-88-7; $Fe(N\text{-pyO})_6(ClO_4)_2$, 23195-10-0.

References and Notes

(1) N. N. Greenwood and T. C. Gibb, "Mossbauer Spectroscopy", Chapman and Hall, New York, N.Y., 1971, Chapter 6.
(2) R. Ingalls, *Phys. Rev. A*, **133**, 787 (1964).
(3) (a) I. Dézsi and L. Keszthelyi, *Solid State Commun.*, **4**, 511 (1966); (b) J. M. D. Coey, I. Dézsi, P. M. Thomas, and P. J. Ouseph, *Phys. Lett. A*, **41**, 125 (1972).
(4) J. Reedijk and A. M. van der Kraan, *Recl. Trav. Chim. Pays-Bas*, **88**, 828 (1969).
(5) The values given for ΔE_Q in Table II of ref 4 are in fact $^1/_2\Delta E_Q$ (J. Reedijk, personal communication), and we have multiplied all such values by 2 in the present paper.
(6) J. R. Sams and J. C. Scott, *J. Chem. Soc., Dalton Trans.*, 2265 (1974).
(7) J. Selbin, W. E. Bull, and L. H. Holmes, *J. Inorg. Nucl. Chem.*, **16**, 219 (1961).
(8) W. F. Currier and J. H. Weber, *Inorg. Chem.*, **6**, 1539 (1967).
(9) J. Reedijk, P. W. N. M. van Leeuwen, and W. L. Groeneveld, *Recl. Trav. Chim. Pays-Bas*, **87**, 1073 (1968).
(10) C. P. Prabhakaran and C. C. Patel, *J. Inorg. Nucl. Chem.*, **32**, 1223 (1970).
(11) The assignment of ν(Sn–O) in DPSO adducts with diorganotin halides also appears to be uncertain.[12]
(12) R. S. Randall, B. V. Liengme, and J. R. Sams, *Can. J. Chem.*, **50**, 3212 (1972).
(13) C. J. Ballhausen, "Introduction to Ligand Field Theory", McGraw-Hill, New York, N.Y., 1962.
(14) For a tetragonal field the e_g orbitals are also split, but they remain degenerate in the case of a trigonal field.
(15) See ref 1, Chapter 3.
(16) J. N. R. Ruddick and J. R. Sams, *J. Chem. Soc., Dalton Trans.*, 470 (1974).
(17) C. E. Johnson, *Proc. Phys. Soc., London*, **92**, 748 (1967).
(18) E. A. Blom, B. R. Penfold, and W. T. Robinson, *J. Chem. Soc. A*, 913 (1969).
(19) N. W. Isaacs and C. H. L. Kennard, *J. Chem. Soc. A*, 1257 (1970).
(20) M. J. Bennett, F. A. Cotton, and D. L. Weaver, *Acta Crystallogr.*, **23**, 581 (1967).
(21) T. C. Gibb, *J. Chem. Soc. A*, 1439 (1968).
(22) We ignore the small fourth-order axial and rhombic terms.
(23) R. M. Golding, "Applied Wave Mechanics", Van Nostrand, Princeton, N.J., 1969.
(24) B. N. Figgis, J. Lewis, F. E. Mabbs, and G. A. Webb, *J. Chem. Soc. A*, 442 (1967).
(25) See, e.g., Y. Hazony, *Moessbauer Eff. Methodol.*, **7**, 147 (1971).
(26) M. G. Clark, *J. Chem. Phys.*, **48**, 3246 (1968).
(27) M. Blume, *Phys. Rev. Lett.*, **14**, 96 (1965).
(28) A. N. Buckley, G. V. H. Wilson, and K. S. Murray, *Solid State Commun.*, **7**, 471 (1969).
(29) B. W. Fitzsimmons and C. E. Johnson, *Chem. Phys. Lett.*, **6**, 267 (1970).
(30) (a) V. I. Gol'danskii, E. F. Makarov, and V. V. Khrapov, *Phys. Lett.*, **3**, 344 (1963); (b) S. V. Karyagin, *Dokl. Akad. Nauk SSSR*, **148**, 1102 (1963).
(31) A preliminary communication on this aspect of the present work has

appeared: J. R. Sams and T. B. Tsin, *J. Chem. Phys.*, in press.
(32) M. G. Clark, G. M. Bancroft, and A. J. Stone, *J. Chem. Phys.*, **47**, 4250 (1967).
(33) R. Zimmermann, H. Spiering, and G. Ritter, *Chem. Phys.*, **4**, 133 (1974).
(34) J. S. Griffith, *Phys. Rev.*, **132**, 316 (1963).
(35) J. S. Griffith, "The Theory of Transition Metal Ions", Cambridge University Press, Cambridge, 1964, pp 355–360.
(36) M. G. Clark, personal communication.
(37) See, e.g., the $\theta = 0$ case in Figure 3.1 of J. R. Sams, *Phys. Chem., Ser. One*, **4**, 85 (1972).

Contribution from the Department of Chemistry,
Tulane University, New Orleans, Louisiana 70118

Synthesis, Spectral Properties, and Reactions of Manganese and Rhenium Pentacarbonyl Phosphine and Phosphite Cation Derivatives and Related Complexes[1]

D. DREW,[2] D. J. DARENSBOURG,* and M. YORK DARENSBOURG

Received December 4, 1974 AIC40813A

The synthesis of a variety of monosubstituted manganese and rhenium carbonyl cationic species of the form $[M(CO)_5L][PF_6]$ is reported, where L = group 5A ligands. Preparation of these derivatives was accomplished either through the reaction of $[LM(CO)_4]^-$ with $C_2H_5O_2CCl$ followed by treatment with HBF_4 (or BF_3) or by thermal replacement of CH_3CN in the $M(CO)_5(CH_3CN)^+$ derivative. The latter procedure was shown to be the method of choice. The reaction of these pentacarbonyl derivatives with CH_3NH_2 to form *cis*-$[Mn(CO)_4(L)C(O)NHCH_3]$ is discussed in relation to other nucleophilic reactions at the carbonyl carbon atom. Displacement of CO ligands from the $Mn(CO)_5(CH_3CN)^+$ species in solution by pyridine, phosphines, and CH_3CN is also reported. In some of these multisubstituted species, exchange of the bound CH_3CN ligands was observed. The CO stretching force constants were calculated for all the cationic species prepared. In the pentacarbonylmanganese phosphine derivatives the axial CO force constant, k_1, was quite similar to the equatorial CO force constant, k_2. This result is discussed in terms of a direct donation of phosphorus σ electrons into the π orbitals of the equatorial CO ligands.

Introduction

The extreme sensitivity of the carbonyl ligand in low-valent transition metal complexes toward subtle changes in electronic and steric environment may be monitored both spectroscopically and chemically. For studies defining the nature and magnitude of these effects the preparation of metal carbonyl derivatives, $L_xM(CO)_y$, where L encompasses a range of ligands of varying electronic and steric properties is a necessity.[3-5] Preparations of neutral mononuclear metal carbonyl derivatives generally involve straightforward substitution processes, utilizing either light or thermal energy for the initial M–C bond cleavage in the parent $M(CO)_{x+y}$. Preparations of charged analogs are however considerably more difficult.

The preparation of cationic manganese carbonyl derivatives of the type $Mn(CO)_5L^+$ (L = a Lewis base), which are isoelectronic with $Cr(CO)_5L$ species, has received little attention. Kruck and Hofler[6] have reported the preparation of a limited number of mono- and disubstituted cationic manganese carbonyl derivatives according to the high-pressure synthesis

$$Mn(CO)_{5-n}L_nCl + AlCl_3 \xrightarrow[CO]{250\ atm} [Mn(CO)_{6-n}L_n][AlCl_4] \qquad (1)$$

where L = PPh_3, $P(c\text{-}C_6H_{11})_3$, and *o*-phenanthroline.

We wish to report the preparation of an extensive series of $Mn(CO)_5L^+$ derivatives (L = $P(OPh)_3$, PPh_3, $P(p\text{-}MeC_6H_4)_3$, PMe_2Ph, diphos, NC_5H_5, CH_3CN) as well as products derived from further CO substitution in these $Mn(CO)_5L^+$ species. The preparation of a few rhenium analogs is also reported. In addition, this synthetic capability has allowed us to carry out several interesting spectral and reactivity investigations.

Experimental Section

Material and Equipment. Tetrahydrofuran was purified by distillation from sodium benzophenone dianion under N_2. All other solvents and reagents were reagent grade and used without further treatment. $Mn_2(CO)_{10}$ was generously supplied by Professor G. R. Dobson. Dimethylphenylphosphine was the generous gift of M and T Chemicals Co. All other phosphines were purchased from Strem Chemical Co. Nitrosyl hexafluorophosphate ($NOPF_6$) was obtained from Alfa Inorganics, Inc.

Melting points were taken in open capillary tubes on a Thomas-Hoover apparatus and are uncorrected. Infrared spectra were taken on a Perkin-Elmer 521 grating spectrophotometer which was calibrated above 2000 cm^{-1} with gaseous CO and below 2000 cm^{-1} with water vapor. The NMR spectra were obtained on a JEOLCO MH-100 instrument.

Preparations. $[LMn(CO)_4]_2$ complexes were prepared from $Mn_2(CO)_{10}$ and ligand (L) using a modified procedure of that previously published by Wawersik and Basolo[7] for the thermal preparation of $[Ph_3PMn(CO)_4]_2$.

$[Ph_3PMn(CO)_4]_2$. $Mn_2(CO)_{10}$ (1.0 g, 2.6 mmol) and 1.33 g (5.2 mmol) of Ph_3P in 20 ml of 1-butanol were refluxed at 120–130° under nitrogen for 2 hr. The initial red solution slowly changed to orange and the orange product precipitated during the heating period. Upon cooling the product was isolated by filtration, washed with pentane, and then recrystallized as orange needles from benzene–heptane. The yield was 1.37 g or 62.5% (mp 133–136° dec and ν(CO) (in $CHCl_3$) 1985 (w) and 1955 (vs) cm^{-1}).

$[(PhO)_3PMn(CO)_4]_2$. $Mn_2(CO)_{10}$ (1.0 g, 2.6 mmol) and 1.6 g (5.2 mmol) of $(PhO)_3P$ in 20 ml of 1-butanol were refluxed at 120–130° under nitrogen for 6 hr. As the solution was cooled to room temperature, a yellow crystalline solid precipitated out. The product was filtered off and recrystallized from CH_2Cl_2–hexane at −78°. The yield was 1.56 g or 65% (mp 136–140° and ν(CO) (in $CHCl_3$) 2003.3 (w, sh) and 1977.8 (vs) cm^{-1}).

$[(CH_3)_2PhPMn(CO)_4]_2$. This previously unreported dimer was prepared in much the same manner as those above from 2.0 g (5.2 mmol) of $Mn_2(CO)_{10}$ and 1.45 g (10.4 mmol) of $(CH_3)_2PhP$ in 20 ml of 1-butanol at 120–130° for 2 hr. Cooling the solution to 0° caused an orange crystalline solid to precipitate. The product was filtered off and recrystallized from benzene–heptane as orange crystals. The yield was 1.62 g or 52% (mp 173–179° and ν(CO) (in $CHCl_3$) 2049.5 (vs), 1980.3 (w), and 1947.3 (vs) cm^{-1}). Anal. Calcd for $C_{24}H_{22}O_8P_2Mn_2$: C, 47.2; H, 3.62; mol wt 610. Found: C, 47.5; H, 3.75; mol wt 586 (determined osmometrically in benzene).

$[CH_3CNMn(CO)_5][PF_6]$. $Mn_2(CO)_{10}$ (7.7 mmol) dissolved in 90 ml of CH_3CN was stirred under N_2 and 1 molar excess (~5 g) of $NOPF_6$ was added to the solution.[8-11] A vigorous reaction occurred immediately with evolution of NO gas. After stirring of the reaction solution for an additional 5 min the volume of the solution was reduced to 30 ml and the product precipitated by the addition of 100 ml of